CHAPTER 4

Biological evaluation

4.1 Introduction

The synthesised 2-aminopyrimidines and their chalcone intermediates were investigated as antagonists of adenosine A_{2A} receptors and inhibitors of the MAO-A and MAO-B enzymes, respectively. The experimental methods and equipment as well as the results of the *in vitro* and *in vivo* evaluations of these compounds are given and discussed in this section.

4.2 Enzyme kinetics

4.2.1 Introduction

Enzyme kinetics is the study of the rate at which an enzyme catalyzes the conversion of substrate to product and is used to determine the potency of the interaction between an inhibitor and a specific enzyme.

Enzymes are protein catalysts that accelerate the rate of a chemical reaction by binding to a substrate and lowering the activation energy needed to convert it to a product. There are several factors that can influence the rate at which an enzyme works, for example:

- The concentration of a substrate [S]
- Temperature
- pH
- The presence of inhibitors
- Activation energies.

In an enzyme catalysed transformation of a substrate (S) to a product (P), the rate limiting step is the breakdown of the Enzyme-Substrate complex (ES) (Figure 4.1)

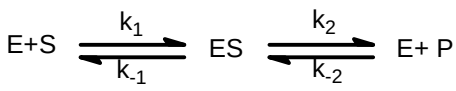

Figure 4.1: Enzyme catalysed transformation

Seeing that the ES concentration cannot easily be measured experimentally, equations like the Michaelis-Menten equation are used as alternative expressions for the determination of the rate of enzymatic reactions.

4.2.2 The Michaelis-Menten equation

This equation is used to illustrate the relationship between the initial reaction velocity (V_i) and substrate concentration [S].

$$\mathbf{V_i} = \frac{\mathbf{V_{max}}[S]}{\mathbf{K_m}+[S]}$$

V_{max} is the maximum value of V_i and K_m the Michaelis-Menten constant, which can be defined as the substrate concentration where V_i equals half of V_{max} (Figure 4.2)

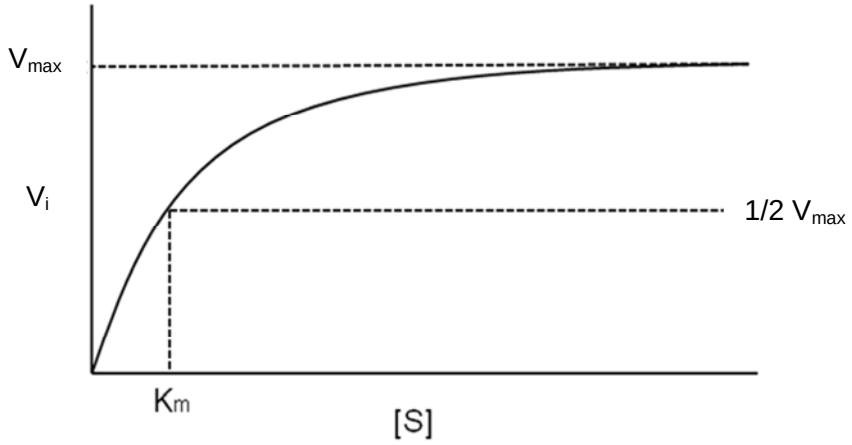

Figure 4.2: Relationship between substrate concentration and the initial velocity of an enzyme-catalyzed reaction.

V_i will almost always be directly proportionate to the enzyme concentration (V_i α [E]) since enzyme activity assays are usually done with an excess substrate over the enzyme. Thus when

the [S] is increased, V_i will follow with increased values until V_{max} is reached. The enzyme is saturated when V_i does not further increase with the increase in [S] (Murray *et al*., 2003).

Under certain circumstances the Michaelis-Menten equation can be reduced to three different forms. Firstly, if the value of K_m is much higher than [S], the expression K_m+ [S] can be replaced by K_m:

$$\mathbf{V_i = \frac{V_{max}[S]}{K_m}}$$

Secondly, if the value of K_m is much lower than that of [S], the term K_m + [S] can be replaced by [S], thus giving:

$$\mathbf{V_i = V_{max}}$$

Lastly, the Michaelis-Menten equation can also be reduced if the values of K_m and [S] are equal. Then V_i can be set equal to half the maximal rate (V_{max}/2) resulting in:

$$\mathbf{V_i = \frac{V_{max}}{2}}$$

Since impractically high concentrations of the substrate are needed to determine V_{max} and K_m, it is not always possible to determine these values with the Michaelis-Menten equation. However, by inverting the Michaelis-Menten equation, the so called Lineweaver-Burk equation is obtained which can be used to determine V_{max} and K_m accurately at very low substrate concentrations.

4.2.3 Lineweaver-Burk equation

$$\mathbf{\frac{1}{V_i} = \left[\frac{K_m}{V_{max}}\right]\frac{1}{[S]} + \frac{1}{V_{max}}}$$

A straight line is obtained when the inverse of both the initial velocity ($1/V_i$) as well as the substrate concentration (1/[S]) are graphically plotted. This straight-line is termed the double reciprocal or Lineweaver-Burk plot (Figure 4.3).

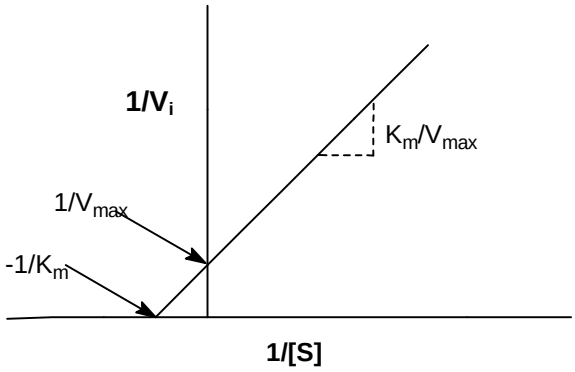

Figure 4.3: Lineweaver-Burk plot.

When examining this plot, it can be seen that the y-axis intercept is equal to $1/V_{max}$, the slope is K_m/V_{max} and the x-axis intercept is equal to $-1/K_m$. Thus, the K_m value may be determined by setting y equal to zero and solving x (Murray *et al*., 2003).

Lineweaver-Burk plots can also be used to determine whether a compound is a competitive or non-competitive inhibitor. Competitive inhibitors bind to the active site of the enzyme and prevent binding of the substrate (and *vice versa*) while non-competitive inhibitors bind to a site other than the active site of the enzyme. This binding by a non-competitive inhibitor then reduces the catalytic activity of the enzyme (Murray *et al*., 2003).

When examining the Lineweaver-Burk plot of a competitive inhibitor, two straight lines (one depicting a situation where no inhibitor is present, and the other where an inhibitor is present) with the same y-intercept will be observed. In this scenario, the V_{max} values will remain unchanged, while the K_m values will vary (Figure 4.4) (Murray *et al*., 2003; Rodwell, 1993).

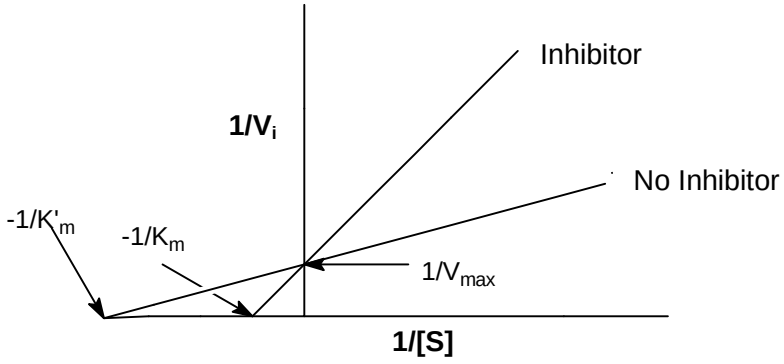

Figure 4.4: Lineweaver-Burk plot indicating competitive inhibition.

After K_m is determined in the absence of an inhibitor, the K_i can be calculated from the following equation.

$$\frac{1}{K_m} = \frac{1}{K_m' + \frac{[I]}{K_i}}$$

K_i can be used to determine the affinity of an inhibitor for the enzyme, since low K_i values are indicative of good potency while higher K_i values signify weaker potency.

With non-competitive inhibition (under the same conditions) the Lineweaver-Burk plot will also show two straight lines but with different y-intercepts and the same x-intercept. The V_{max} values will thus vary and the K_m values will stay the same (Figure 4.5) (Murray *et al*., 2003; Rodwell, 1993).

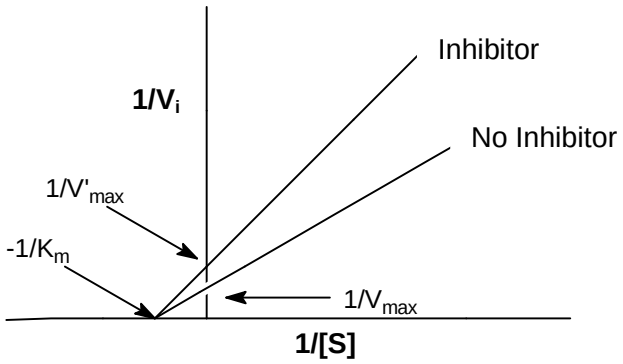

Figure 4.5: Lineweaver-Burk plot indicating non-competitive inhibition.

4.2.4 IC_{50} value determination

IC_{50} values are another way to measure the effectiveness of an inhibitor. IC_{50} is defined as the concentration of the inhibitor that produces 50% inhibition of the enzyme. The following equation illustrates the relationship between the IC_{50} value and K_i (Cheng & Prusoff, 1973).

$$K_i = \frac{IC_{50}}{\left(1 + \frac{[S]}{K_m}\right)}$$

In this study IC_{50} values will be used to express MAO inhibition potencies.

4.3 Biological evaluation of MAO inhibitors.

4.3.1 Introduction

In this study selected chalcone intermediates synthesised in chapter 3 were investigated as inhibitors of MAO-A and -B. For this purpose a fluorometric method, using the mixed MAO-A/B substrate kynuramine, was employed (Novaroli *et al.*, 2005). Several other methods exist, such as the horse radish peroxidase assay (where H_2O_2 formation is measured indirectly) (Zhou & Panchuk-Voloshina, 1997). The kynuramine assay has the advantage that the fluorescence of the 4-hydroxyquinoline product, formed during the oxidation by MAO, can be directly measured, resulting in increased sensitivity (Figure 4.6). The amount of 4-hydroxyquinoline formed is thus measured with a fluorescence spectrophotometer (excitation wavelength of 310 nm, emission wavelength of 400 nm) where after catalytic activity of both MAO-A and -B can be determined.

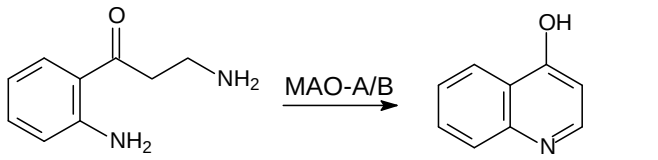

Kynuramine **4-Hydroxyquinoline**

Figure 4.6: The oxidation of kynuramine to 4-hydroxyquinoline.

4.3.2 Materials and methods

Tabel 4.1: Suppliers of reagents and materials used for the assay.

Materials	Company
Recombinant human MAO-A and -B (5 mg/ml), expressed in microsomes	Sigma Aldrich
Kynuramine	Sigma Aldrich
Dimethyl sulfoxide (DMSO)	Riedel-de Haën
Sodium hydroxide (NaOH)	Merck
KH_2PO_4	Merck
K_2HPO_4	Merck
KCl	Merck

Recombinant human MAO-A and -B, expressed in microsomes from baculovirus infected BTI insect cells, were used for these assays. Potassium phosphate buffer (100 mM, pH 7.4, made isotonic with KCl, 20.2 mM) was used for all the enzyme reactions and dilutions. The final volume of the enzyme reactions was 500 µl, and each reaction contained kynuramine (45 µM for MAO-A and 30 µM for MAO-B), various concentrations of the test inhibitors (0, 0.003, 0.01, 0.1, 1, 10 and 100 µM), and 4% DMSO as co-solvent. The reactions were started with the addition of MAO-A or –B (0.0075 mg protein/ml) and then incubated in a waterbath at 37 ºC for 20 minutes. The reactions were subsequently terminated by the addition of 400 µl NaOH (2 N). Water (1000 µl) was added to each reaction, the reactions were centrifuged at 16,000 *g* (10 min) and the concentrations of MAO generated 4-hydroxyquinoline in the supernatants were measured by fluorescence spectrophotometry (λ_{ex} 310 nm; λ_{em} 400 nm).

For the concentration calculations, linear calibration curves were constructed by measuring the fluorescence of samples containing known amounts of 4-hydroxyquinoline (0.047 – 1.56 µM) dissolved in potassium phosphate buffer (500 µl). To each calibration sample NaOH (2 N, 400 µl) and water (1000 µl) were added. For each inhibitor evaluated, the appropriate control samples were analysed in order to confirm that the test inhibitors do not fluoresce or quench the fluorescence of 4-hydroxyquinoline under the assay conditions. From the enzyme rate data, sigmoidal dose response curves (plots of the initial rates of kynuramine oxidation versus the logarithm of inhibitor concentration) were constructed. For the construction of each sigmoidal curve, at least six different inhibitor concentrations were employed, and the inhibitor concentrations covered at least three orders of magnitude. IC_{50} values were estimated from the sigmoidal curves with aid of the Prism 5 software package (GraphPad), employing the one site competition model. IC_{50} values were determined in triplicate and are expressed as mean ± standard deviation (SD). Suppliers of reagents are indicated in Table 4.1.

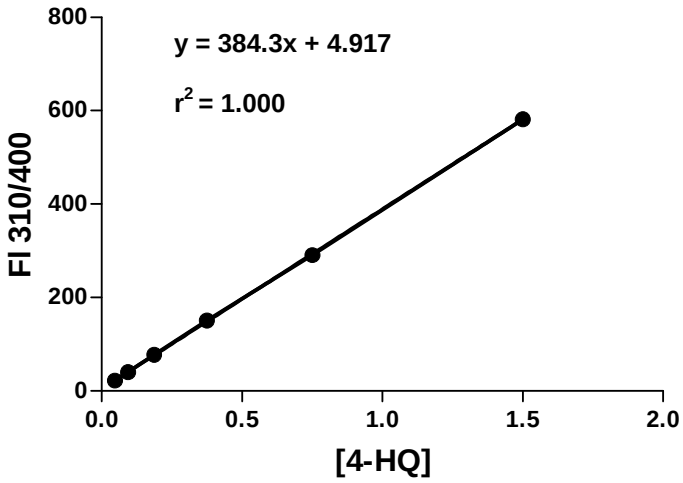

Figure 4.7: Example of a calibration curve routinely obtained

4.3.3 Results

The chalcone intermediates (**1a** -**1h**) were screened for MAO inhibitory activity. Chalcones (**38** and **39**), closely related to the phenylamide derivatives (**1j** – **1n**) did not exhibit any MAO inhibitory activity, possibly because of their larger size preventing them from fitting into the active site. Therefore the MAO inhibitory activities of **1j** – **1n** were not determined.

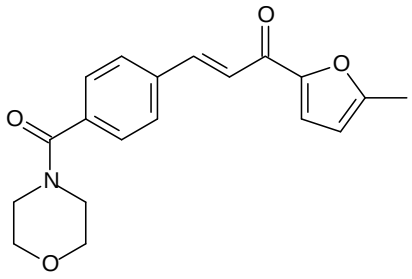

38

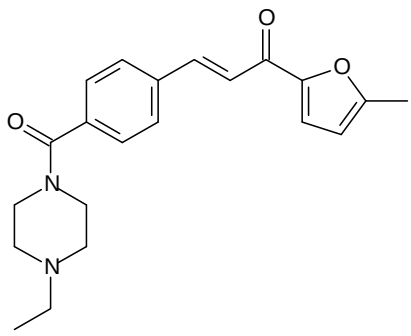

39

The IC_{50} values for the inhibition of MAO-A and -B by selected chalcones are presented in Table 4.2. The lower the IC_{50} value, the higher the binding affinity of the inhibitor for the enzyme. The selectivity index (SI) represents the selectivity of inhibition of MAO-A and MAO-B. The higher this value the more selective the inhibitor is towards the MAO-B enzyme. SI for each compound is calculated by dividing the IC_{50} value of MAO-A by the IC_{50} value for MAO-B.

Table 4.2: MAO inhibitory activities determined for selected chalcones

Compound		IC_{50} (μM)		
		[a]MAO-A	[a]MAO-B	[b]SI
1a.	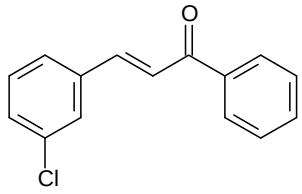	[c]No inhibition	0.529 ± 0.034	[d]-
1b.	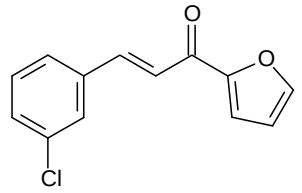	21.1 ± 3.42	2.10 ± 0.142	10.05
1c.	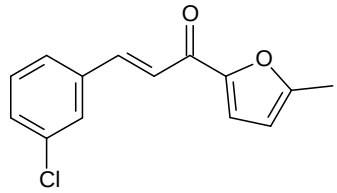	18.0 ± 5.46	0.490 ± 0.064	52.85
1d.	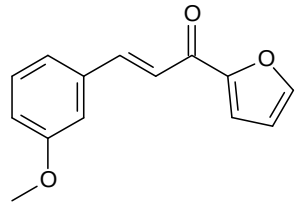	19.2 ± 4.21	3.20 ± 0.37	6.01
1e.	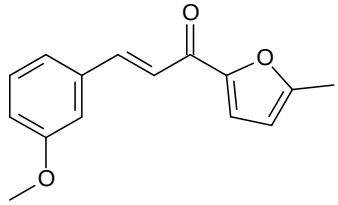	No inhibition	2.79 ± 0.84	-
1f.	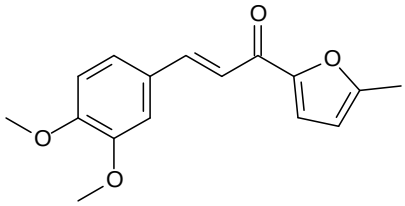	The colour of this compound interferes with the fluorescence measurement of the assay. IC_{50} could therefore not be determined		
1g.	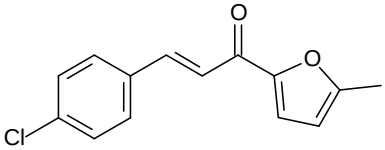	40.9 ± 46.6	0.616 ± 0.047	66.49

1h.	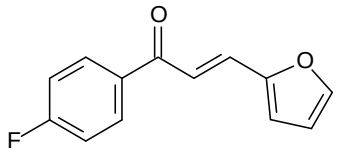	41.8 ± 3.11	7.67 ± 0.688	5.46

[a] *All values are expressed as the mean ± SD of triplicate determinations.*
[b] *The selectivity index is the selectivity for the MAO-B isoform (IC_{50} MAO-A / IC_{50} MAO-B).*
[c] *No inhibition observed at a maximal tested concentration of 100 µM.*
[d] *Not calculated as MAO-A inhibitory value was not available.*

From the results above the following general observations and conclusions can be made:

- The selected chalcones exhibited moderate to good inhibitory activities towards MAO-B, but showed weak or no inhibition of MAO-A.
- The screened chalcones are thus selective for MAO-B, for instance, compound **1g** is 66 times more selective as an inhibitor of MAO-B than MAO-A. It was not possible to calculate a selectivity index for compounds **1a** and **1e**, as no inhibition of MAO-A was observed at the highest concentrations tested, indicating a high degree of selectivity for these compounds in particular.
- Compounds **1a**, **1c** and **1g** exhibited promising MAO-B inhibitory activities, with IC_{50} values in the submicromolar range. However, the most potent compound (**1c**) is at least 5 times less potent than the known selective reversible MAO-B inhibitor lazabemide (IC_{50} = 0.091 µM, as determined in our labarotories under similar assay conditions).
- To obtain a comparison between the effect of furan, phenyl and methylfuran substitution on position 1, the MAO-B activities of compounds **1a** – **1c**, as well as **1d** and **1e** were compared. For compounds **1a** and **1c**, similar activities were obtained. These are the phenyl (**1a**) and methylfuran (**1c**) substituted derivatives. The furan substituted derivative (**1b**) was approximately fourfold weaker as an inhibitor of MAO-B. The same trend was however not observed for the methoxy derivatives (**1d** and **1e**), as furan and methylfuran substitution resulted in compounds with similar MAO-B inhibitory activity.
- The results show that substitution with the electron withdrawing chlorine group results in better MAO-B activity than obtained with the electron donating methoxy (OCH_3) group (compound **1b** vs **1d** and compound **1c** vs. **1e**).
- Of all the compounds screened, compound **1h** exhibited the weakest MAO-B inhibitory activity. Whether this is due to the fluorine substitution on the phenyl ring, or to the change in the positions of the double bond and carbonyl group, is not clear and this needs to be investigated further.

This was a relatively small series of chalcones and the observations and conclusions made here are thus preliminary. Before any final conclusions can be made with regard to the MAO-B activities of furan substituted chalcones, this series will have to be expanded. It should, however, be noted that compound **1a**, **1c** and **1g** are promising MAO-B inhibitors and suitable lead compounds for the future design of MAO-B selective inhibitors.

4.4 Reversibility studies

4.4.1 Introduction

Once it was determined that most of the synthesised chalcones were MAO-B selective inhibitors, the next step was to establish whether the binding of these compounds to the target enzyme was reversible (non-covalent) or irreversible (covalent). The most potent inhibitor (compound **1c**) was selected for this study and the reversibility of binding to the MAO-B enzyme was determined. This was done by measuring the recovery of enzymatic activity after dilution of the enzyme-inhibitor complex. The concentrations of inhibitor screened was 0, 10 and 100% of the IC_{50} value and for these concentrations enzymatic activity has to be recovered to approximately 100, 90 and 50% respectively, if the compound is a reversible inhibitor. If an inhibitor is irreversible, like deprenyl, 0% recovery of enzyme activity is expected even at 10% of the IC_{50} value.

The substrate used was kynuramine which, as mentioned earlier, is metabolised to 4-hydroxyquinoline by MAO-B. The amount of 4-hydroxyquinoline formed is measured spectrofluorometrically, after the incubation and dilution of the three different concentrations of the enzyme-inhibitor complex, as well as incubation and dilution of an enzyme-deprenyl complex (control).

4.4.2 Materials and methods

Table 4.3: Suppliers of reagents and materials used for the assay.

Materials	Company
Recombinant human MAO-A and -B (5 mg/ml)	Sigma Aldrich
Kynuramine	Sigma Aldrich
Dimethyl sulfoxide (DMSO)	Riedel-de Haën
(*R*)-Deprenyl	Sigma Aldrich
NaOH	Merck

Compound **1c** [IC_{50} (MAO-B) = 0.49 µM] at 10 × IC_{50} and 100 × IC_{50} was preincubated with recombinant human MAO-B (0.75 mg/ml) for 30 minutes at 37 ºC. The reaction solvent was potassium phosphate buffer (pH 7.4, 100 mM, made isotonic with KCl). DMSO (4%) served as co-solvent in all preincubations. A control reaction was also carried out in the absence of inhibitor. The reactions were subsequently diluted 100-fold with the addition of kynuramine to yield final concentrations of kynuramine equal to 30 µM, and of MAO-B equal to 0.0075 mg/ml. The final concentrations of **1c** were 0.1 × IC_{50} and 1 × IC_{50}. The reactions were incubated for a further 20 minutes at 37 ºC, terminated and the residual rates of 4-hydroxyquinoline formation were measured as previously described. For comparison, (*R*)-deprenyl (IC_{50} = 0.079 µM) was similarly preincubated with MAO-B at 10 × IC_{50} and diluted 100-fold with the addition of kynuramine to yield a final concentration of (*R*)-deprenyl equal to 0.1 × IC_{50}.

4.4.3 Results

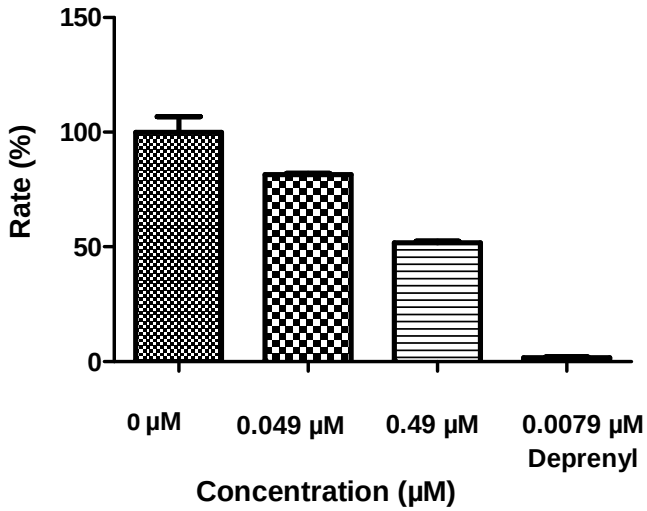

Figure 4.8: Reversibility of inhibition of recombinant human MAO-B by compound **1c**. The enzyme was preincubated with **1c** at 10 × IC_{50} and 100 × IC_{50} for 30 minutes and then diluted to 0.1 × IC_{50} and 1 × IC_{50}, respectively. As control, MAO-B was also preincubated with (*R*)-deprenyl at 10 × IC_{50} and subsequently diluted to 0.1 × IC_{50}. The residual enzyme activities were subsequently measured.

The reversible interaction of **1c** with MAO-B was investigated by evaluating the recovery of enzymatic activity after dilution of the enzyme-inhibitor complex. The results are given in Figure 4.8 and show that, after dilution to 0.1 × IC_{50} (0.049 µM) and 1 × IC_{50} (0.49 µM), the MAO-B catalytic activities were recovered to approximately 80% and 50% respectively, of the control

value. It is expected that, for reversible inhibitors, catalytic activity of MAO-B will recover to levels of approximately 90% and 50% after diluting the inhibitor concentration to 0.1 × IC_{50} and 1 × IC_{50}, respectively. After preincubation of MAO-B with the irreversible inhibitor (*R*)-deprenyl (at 10 × IC_{50}), and dilution of the resulting complex to 0.1 × IC_{50}, MAO-B activity is not recovered (1% of control). These data indicate that **1c** interacts reversibly with MAO-B. Interestingly, after dilution, the enzyme activities are not recovered to 90% and 50%, respectively, as expected.

4.5 Mode of inhibition - Construction of Lineweaver-Burk plots

4.5.1 Introduction

This study is used to determine whether a compound's inhibition is competitive or non-competitive. Compound **1c** was again selected for evaluation as it is the most potent MAO-B inhibitor of the series. To determine the mode of inhibition of **1c**, Lineweaver-Burk plots were constructed and the mode of inhibition was determined from the appearance of these plots.

4.5.2 Method

The mode of MAO-B inhibition was investigated with the aid of a set of four Lineweaver-Burk plots. The first plot was constructed in the absence of inhibitor while the remaining three plots were constructed in the presence of different concentrations of inhibitor. For this study, compound **1c** was selected as representative inhibitor at the following concentrations: 0, 0.12, 0.25 and 0.49 µM. Kynuramine at concentrations of 15, 30, 60 and 90 µM served as substrate and recombinant human MAO-B was used at a concentration of 0.015 mg/ml. The rates of formation of the MAO-B generated 4-hydroxyquinoline were measured by fluorescensce spectrophotometry as previously described. Linear regression analysis was performed using Prism 5.

4.5.3 Results

Figure 4.9 illustrates the set of Lineweaver-Burk plots that were obtained from these studies. The results show that the Lineweaver-Burk plots are linear and intersect at the y-axis. This indicates that the inhibition of MAO-B by **1c** is competitive.

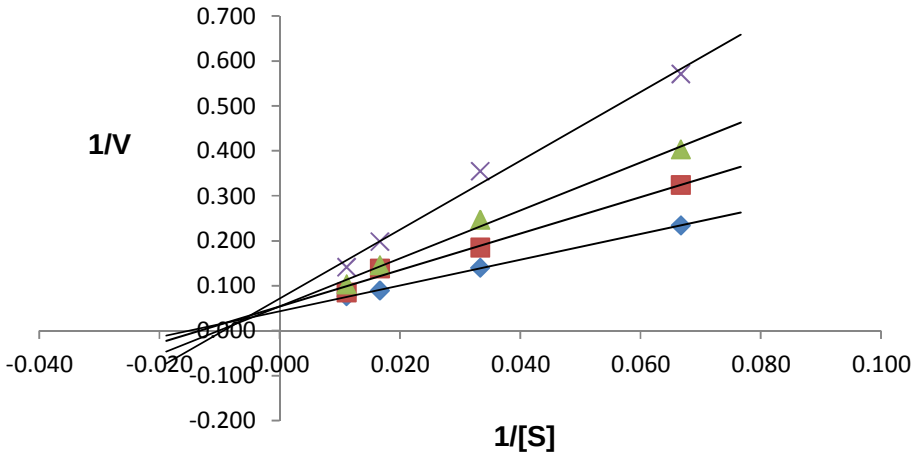

Figure 4.9: Lineweaver-Burk plots of the oxidation of kynuramine by recombinant human MAO-B. The plots were constructed in the absence (blue diamonds) and presence of various concentrations of compound **1c**. The concentrations of compound **1c** employed were: 0.1225 µM (red squares), 0.245 µM (green triangles), 0.49 µM (purple crosses). The rates (V) are expressed as nmol product formed/min/mg protein.

4.6 Biological evaluation of 2-aminopyrimidines as adenosine A_{2A} antagonists

4.6.1 Introduction

To determine whether the 2-aminopyrimidines have affinity for the adenosine A_{2A} receptor, a radioligand binding assay was used. The non-selective adenosine antagonist, [^{3}H]5'-N-ethylcarboxamide-adenosine ([^{3}H]NECA), which binds to both the adenosine A_{2A} and A_1 receptors, was employed as the radioligand. Binding was determined in the presence of N^6-cyclopentyladenosine (CPA), since it is a selective adenosine A_1 agonist that displaces [^{3}H]NECA from the A_1 receptor. [^{3}H]NECA can thus only bind to the A_{2A} receptor and the radioactivity measured is an indication of binding only to the A_{2A} receptor. If a test compound has affinity for the A_{2A} receptor it will displace the [^{3}H]NECA and the measured radioactivity (CPM) would be low. If the compound has weak or no affinity for the A_{2A} receptor the measure radioactivity (CPM) would be high (as discussed in section 2.5.2.6).

4.6.2 Materials and methods

Tabel 4.4: Suppliers of reagents and materials used for the assay.

Materials	Company
Adenosine deaminase (250 units)	Sigma Aldrich
N^6-Cyclopentyladenosine (CPA)	Sigma-Aldrich
Dimethyl sulfoxide (DMSO)	Riedel-de Haën
25 *Ci/mmol (250 µCi) [^{3}H]5'-N-ethylcarboxamide-adenosine ([^{3}H]NECA)	Amersham Biosciences
Filtercount scintillation fluid	Sepsi
Magnesium chloride anhydrous	Sigma-Aldrich
Silicone solution (Sigma-cote)	Sigma Aldrich
Trizma® Base	Fluka
Trizma® Hydrochloride	Fluka
Whatman® GF/B 25 mm diameter filters	Merck

*Curies per millimole

Tissue preparation for binding studies

The Animal Research Ethics Committee of the North-West University (NWU-0035-10-A5) approved the collection of animal tissue required for this assay. Male Sprague Dawley rats (approximate weight 500 g) were obtained from the Animal Research Center of the North-West University, Potchefstroom campus. Striata were dissected from rat brains. These were kept on ice during the dissection and immediately snap frozen with liquid nitrogen and stored at -70˚C.

The frozen striata were suspended in 10 ml of ice-cold 50 mM Tris (kept on ice) and disrupted for 30 seconds with a Polytron PT-10 homogeniser (Brinkman) at a setting of 5. The suspension was centrifuged for 10 minutes at 50, 000 × g. The supernatant was decanted and the pellet resuspended in 10 ml ice-cold Tris buffer. This suspension was then homogenised and centrifuged as before and the final pellet was suspended in ice-cold Tris to yield a 1 g/5 ml suspension. The membrane suspension was aliquoted (790 µl membrane per microcentrifuge tube) and stored at -70˚C. Three tubes were used per assay.

Preparation of membrane suspension

Magnesium chloride ($MgCl_2$, 48.21 mg), adenosine deaminase (9.36 µl) and the prepared striatal membranes (0.474 g) were added to a tube containing 40 ml Tris buffer. The tube was vortexed for 5 seconds after the addition of each item. This suspension was kept on ice during the assay.

Binding study

The procedure used in the assay was adapted from Bruns *et al*., (1986). Tris buffer (pH 7.7) was used for all incubations. A stock solution of CPA (N^6-cyclopentyladenosine, 10 mM) was prepared in DMSO and diluted to 500 nM in Tris buffer on the day of the experiment. [^{3}H]NECA was diluted in Tris buffer to obtain a 40 nM solution. Test compounds were dissolved in DMSO on the day before the experiment and diluted further to 100 times the final incubation concentration. All pipette points and plastpro tubes used during the assay were coated with sigmacote®.

The final volume of the incubations was 1000 µl and each incubation contained test compound (0-100 µM), membrane suspension as prepared above (containing ~10 mg of original tissue weight of rat striata), CPA (50 nM) and [^{3}H]NECA (4 nM). For incubations, the order of additions was test compound (10 µl), membrane suspension (790 µl) CPA (100 µl) and [^{3}H]NECA (100 µl). All incubations were done in duplicate in 4 ml tubes. Non-specific binding was determined in triplicate by adding the following (in this particular order): membrane suspension (790 µl), CPA (100 µl, final concentration 50 nM), [^{3}H]NECA (100 µl, final concentration 4 nM), and CPA (10 µl, final concentration 100 µM). After addition of the reagents, all tubes were vortexed and incubated for 30 minutes at 25 ˚C in a shaking waterbath (70 min^{-1}). All tubes were then again vortexed and incubated for a further 30 minutes. The incubations were terminated with rapid filtration through Whatman® GF/B 25 filters (25 mm diameter) fitted on a Hoffeler vacuum system and washed twice with 4 ml ice cold Tris. The damp filters were placed into scintillation vials and scintillation fluid (4 ml) was added. The vials were shaken thoroughly and left for 2 h. A Packard Tri-CARB 2100 TR scintillation counter was used to count the radioactivity retained on the filters. Specific binding was defined as total binding minus nonspecific binding, and was expressed as counts per minute (CPM).

Data analysis

By using the one site competition model of the Prism 5 software package (GraphPad) the CPM values were plotted against the logarithm of the inhibitor concentration to give a sigmoidal dose-response curve that was used to calculate the IC_{50} values.

The equation for the calculation of IC_{50} value with non-linear regression is as follows:

$$\mathbf{Y = Bottom + \frac{Top - Bottom}{1 + 10^{x - \log IC_{50}}}}$$

Where Y is the CPM, representing radioligand binding, and X is the concentration of unlabeled ligand. "Top" and "Bottom" represents the top and bottom part of the sigmoidal curve, respectively.

K_i values were calculated from the IC_{50} values by using the Cheng-Prusoff equation (Cheng & Prusoff, 1973), as applicable to radioligand binding assays, indicated below.

$$\boldsymbol{K_i = \frac{IC_{50}}{\left(1 + \frac{[L]}{K_d}\right)}}$$

Where L is the concentration of the radioligand ([^{3}H]NECA, 4 nM). K_d is the equilibrium dissociation constant for the radioligand under the same conditions as in the assay, and was taken as 8.5 nM (Müller *et al*., 1993).

As mentioned earlier, incubations were carried out in duplicate and both the IC_{50} and K_i values are given in Table 4.5. These values are expressed in nM, where a low K_i value indicates good affinity and a higher value indicates weak affinity for the receptor. The binding affinity of the known adenosine A_{2A} antagonists, KW 6002 and ZM 245381 were determined to ensure the validity of the assay.

4.6.3 Results

The sigmoidal dose-response curves for compounds **2m** and **2j**, which were used to determine their respective IC_{50} values are given in Figure 4.10. These dose-response curves are given as example of data routinely obtained in this study. As mentioned before, all IC_{50} values were measured in duplicate.

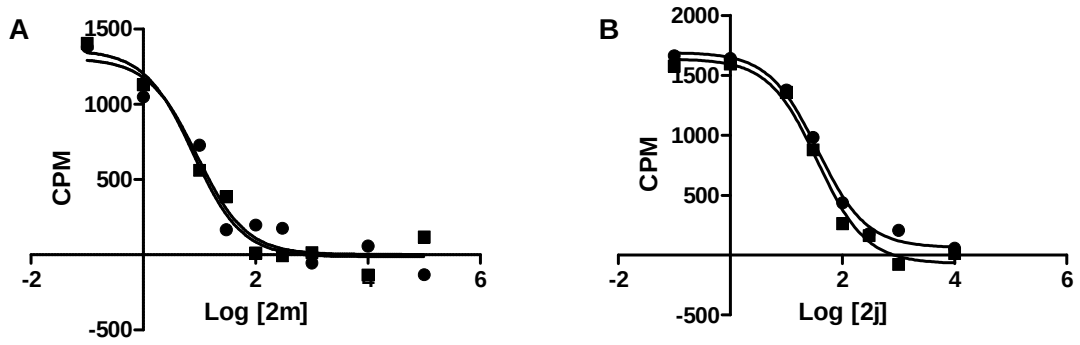

Figure 4.10: (A) The sigmoidal dose-response curve of CPM versus logarithm of the concentration of compound **2m** with a IC_{50} value of 8.47 nM which corresponds to a K_i value of 5.76 nM. (B) The sigmoidal dose-response curve of compound **2j**. The calculated IC_{50} value is 26.6 nM which corresponds to a K_i value of 19.8 nM.

The IC_{50} and calculated K_i values, for the affinity of the synthesised 2-aminopyrimidines for rat striatal A_{2A} receptors, are shown in Table 4.5.

Table 4.5: Adenosine A_{2A} receptor affinity of synthesised 2-aminopyrimidines and the known antagonist ZM 241385

	Compound	[a]K_i (nM)	[a]IC_{50} (nM)
2a.	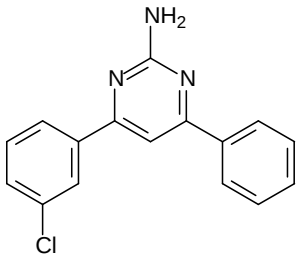	861 ± 180	1265 ± 265
2b.	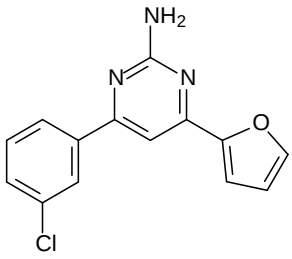	223 ± 27.0	328 ± 39.7

Compound		[a]K_i (nM)	[a]IC_{50} (nM)
2c.	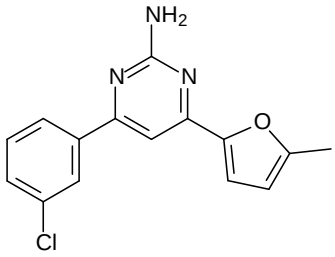	362 ± 193	532 ± 284
2d.	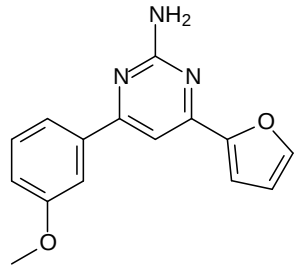	226 ± 102	332 ± 150
2e.	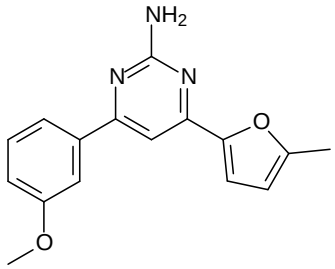	371 ± 279	545 ± 410
2f.	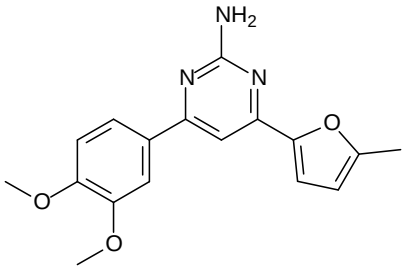	2520 ± 481	3706 ± 708
2g.	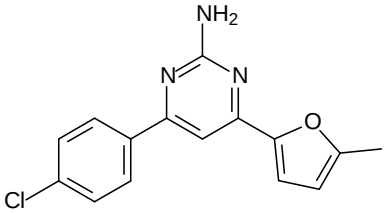	3012 ± 621	4430 ± 914

Compound		[a]K_i (nM)	[a]IC_{50} (nM)
2h.	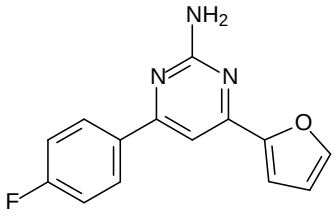	233 ± 46.6	342 ± 68.6
2j.	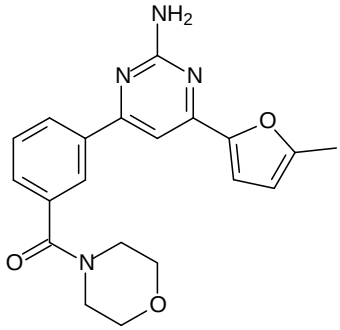	26.6 ± 1.26	39.1 ± 1.85
2k.	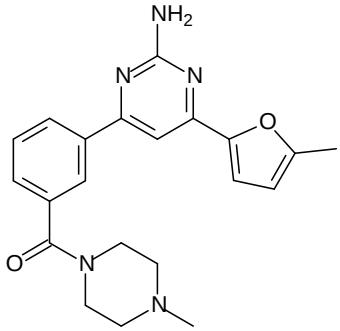	14.8 ± 2.80	21.7 ± 4.12
2l.	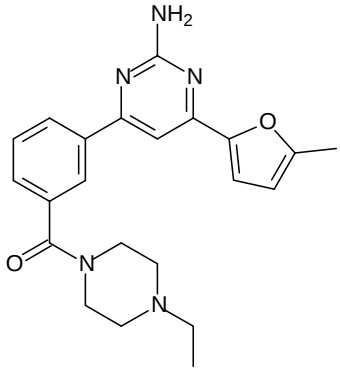	28.0 ± 3.98	41.2 ± 5.86

Compound		[a]K_i (nM)	[a]IC_{50} (nM)
2m.	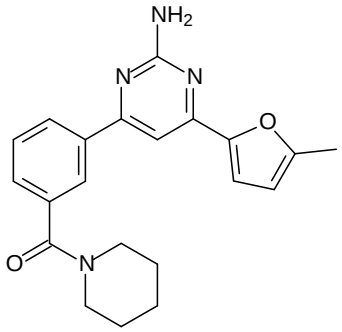	5.76 ± 0.68	8.47 ± 1.00
2n.	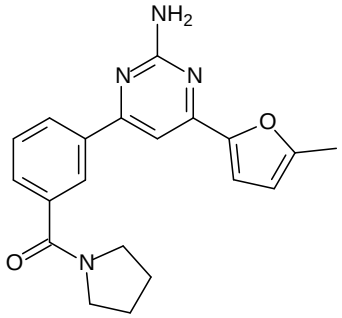	52.8 ± 25.6	77.7 ± 37.6
ZM 241385	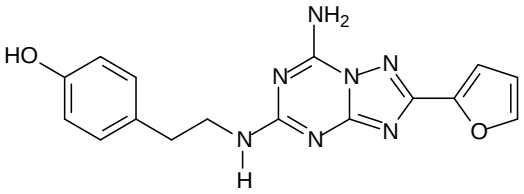	[b]2.10 ± 1.78	3.09 ± 2.61
KW 6002	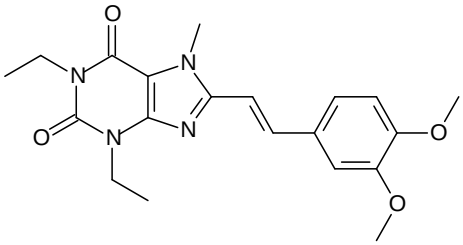	[c]10.3 ± 5.21	15.1 ± 7.66

[a]*All values are expressed as the mean ± SD of duplicate determinations.*
[b]*Literature K_i value for ZM 241385 is reported as 2 nM* (Müller & Ferré, 2007*)*
[c]*Literature K_i value for KW 6002 is reported as 5.15 nM* (Müller & Ferré, 2007)

From these results the following observations were made with regard to the binding affinities of compounds **2a** - **2h** to adenosine A_{2A} receptors:

- These derivatives exhibited moderate to weak affinities for the A_{2A} receptor with K_i values ranging from 226 nM (**2d**) – 3012 nM (**2g**).
- Replacing the phenyl substituent in position 6 with either a furan or methylfuran group, results in improved affinity (compound **2a** vs. compounds **2b** and **2c**).

- When the affinities of compounds **2b** and **2c**, and compounds **2d** and **2e** are compared, it appears that methyl substitution of the furan ring results in decreased affinity (approximately 1.6 times).
- The affinity is apparently not affected by the electronic effects of the substituent on the phenyl ring as compounds **2b** and **2d** (with K_i values of approximately 250 nM) as well as compounds **2c** and **2e** (with K_i values of approximately 400 nM) had similar affinities for A_{2A} receptors.
- On the other hand, the position of the substituent on the phenyl ring seems to have a significant effect on the affinity, where chlorine substitution on the 4-position (**2g**) results in much weaker binding than chlorine on the 3-position (**2c**). A similar observation was made when the affinities of compounds **2e** and **2f** were compared, where addition of another methoxy substituent in position 4 resulted in much weaker affinity.
- The affinity of compound **2h**, with a 4-fluorophenyl substituent, was better than that observed for compound **2g**, with 4-chlorophenyl substituent. Size of the substituent may thus also play a role in the binding of this class of compounds to A_{2A} receptors. Further investigation is required to clarify this point.

Furthermore, for the compounds **2j** - **2n** the following was observed:

- Generally, the phenylamide derivatives (**2j** - **2n**) have higher affinities than the derivatives substituted with simple electron withdrawing and donating groups (**2a** - **2h**), which exhibited moderate to poor affinities for the A_{2A} receptor.
- The most promising candidate was compound **2m**, with a K_i value of 5.76 nM. This value is comparable to the measured K_i values of the known A_{2A} receptor antagonists ZM 241385 (K_i = 2.10 nM) and KW 6002 (10.3 nM).
- Different amide substituents on the 3-position of the phenyl ring yielded compounds with different affinities for the A_{2A} receptor. The sequence of affinity of amine groups in this position is piperidine > methylpiperazine > morpholine = ethylpiperazine > pyrrolidine.

In order to rationalise the differences in the observed affinities among the members of this class of compounds, the docking experiments as performed in Chapter 3, were revisited.

The selected poses (see chapter 3) of the docked 2-aminopyrimidines were ranked according to C-DOCKER_INTERACTION energies. Interestingly, in all cases, the phenylamide derivatives (**2j** - **2n**) ranked above the compounds substituted with various electron donating and

withdrawing groups (**2a** - **2h**). This indicates that the interaction between the amide derivatives and the receptor is energetically more favourable than that obtained with the "smaller" aminopyrimidines, and provides, at least in part, an explanation for the observed superior affinity of these particular derivatives for the A_{2A} receptor.

Careful consideration of the interactions of the aminopyrimidines and the receptor, further revealed the following: All of the derivatives (**2a** – **2n**), undergo hydrogen bonding interactions with Glu 169 and Asn 135, while the three membered ring system forms pi interactions with Phe 168, as mentioned before. This anchors the aminopyrimidine in the active site and is also an important binding interaction seen in other antagonists (see chapter 3). However, for the phenylamide derivatives (**2j** - **2n**), an additional hydrogen bonding interaction is observed between the amide carbonyl group and Tyr 271 (Figure 4.11). It is hypothesised that this additional structural feature (the amide carbonyl) is therefore a major contributing factor to the differences observed in affinities between these two sets of aminopyrimidines.

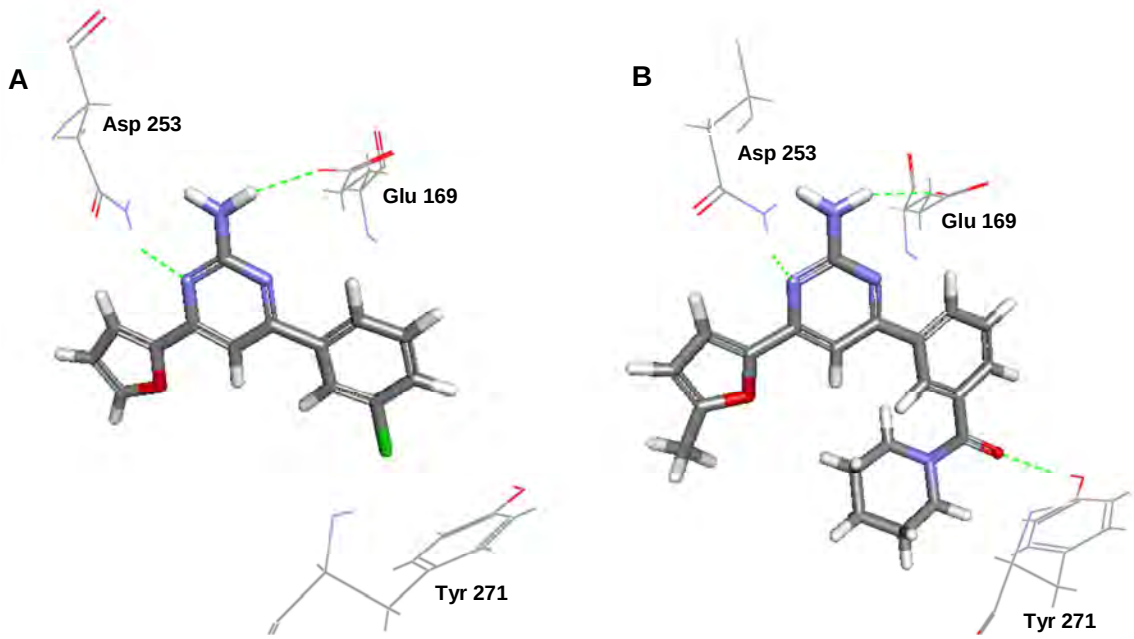

Figure 4.11: (A) Illustration of the intermolecular hydrogen bond interactions of compound **2b**. (B) Illustration of the additional intermolecular hydrogen bond interaction between the amide carbonyl of compound **2m** and Tyr 271.

4.7 *In vivo* assays

Since promising affinities to A_{2A} receptors were obtained in the radioligand binding assay for both compounds **2m** (K_i = 5.76 nM) and **2k** (K_i = 14.8 nM), these compounds were selected for further *in vivo* studies.

4.7.1 Introduction

In this part of the study, the ability of a compound to act as an antagonist of the adenosine A_{2A} receptor is assessed. The reversal of haloperidol induced catalepsy (discussed in Chapter 2 paragraph 2.5.2.6), is measured with the standard bar test. The rationale behind the reversal of catalepsy by an A_{2A} antagonist can be explained by considering the second messenger system. The dopamine D_2 receptors and adenosine A_{2A} receptors are Gi and Gs coupled receptor subtypes that inhibit and stimulate cAMP levels, respectively. The administration of the dopamine D_2 antagonist haloperidol will result in increased cAMP levels as the inhibitory effects of the D_2 receptors are abolished and the stimulatory effects of the A_{2A} receptor still remain unopposed. This increased cAMP level induces catalepsy. The administration of an adenosine A_{2A} antagonist will halt the stimulatory effects of the A_{2A} receptors, cAMP levels will decrease and catalepsy will be reduced.

4.7.2 Methods

4.7.2.1 Animals

Thirty male (n = 30) Sprague-Dawley rats were obtained and housed in groups of six animals per cage. These animals were given free access to standard laboratory food and water until the required weight was obtained (240 g - 300 g). All efforts were made to minimise animal suffering as experiments were carried out in accordance with the National Institute of Health's Guide for the Care and Use of Laboratory Animals. The experimental protocol was approved by the North-West University ethical committee (NWU-00035-10-S5).

4.7.2.2 Compounds

Haloperidol (Serenace Injection; 5 mg/ml)

To induce catalepsy a dose of 5 mg/kg haloperidol was administered (Trevitt *et al*., 2009).

KW 6002

A vehicle control solution (50 ml) was prepared by mixing a 1:1:4 solution of DMSO, Tween 80 and saline. The test compound was dissolved in a required amount of control solution to yield concentrations of 0.1, 0.4, 1 and 2 mg/ml. A suitable volume of these solutions was injected

depending on the weight of the rat, resulting in final dose concentrations of 0.1, 0.4, 1 and 2 mg/kg. This compound was included in the study to determine assay validity.

*Aminopyrimidines (**2k** and **2m**)*

A vehicle control solution (50 ml) was prepared by mixing a 1:1:4 solution of DMSO, Tween 80 and saline. The test compound was dissolved in a required amount of control solution to yield concentrations of 0.1, 0.4, 1 and 2 mg/ml. A suitable volume of these solutions was injected depending on the weight of the rat, resulting in final dose concentrations of 0.1, 0.4, 1 and 2 mg/kg. All injections were intraperitoneally (i.p.).

4.7.2.3 Catalepsy test

The experiments were carried out between 8:00 and 15:30 in a lit room with a controlled temperature. All the rats were drug naïve and were only used once. Haloperidol-induced catalepsy was measured with the standard bar test, in a Perspex chamber (length, 23 cm; width, 10.5 cm; height, 9 cm) with a horizontal plastic bar (diameter, 1 cm; length, 10.5 cm) fixed at 9 cm above the floor, and at 7 cm from the back of the box (Figure 4.12).

Figure 4.12: Cataleptic rat placed with its front paws on the horizontal bar

Animals were divided into 5 groups, (control 0, 0.1, 0.4, 1 and 2 mg/kg groups) each group containing 6 rats. All rats received i.p injections of haloperidol 5.0 mg/kg to induce catalepsy. Thirty minutes later, the rats in each group received i.p injections of the corresponding concentration of test compound. The vehicle control solution was administered to rats in the control group. Catalepsy was measured 60 minutes after the haloperidol injections by placing the rats in the Perspex box with their front paws on the horizontal bar (as in Figure 4.12). Catalepsy was measured as the time the animal maintained its position on the bar. Time was recorded until one or both of the rat's front paws were removed from the bar, or up to 120 seconds.

Groups were as follows:
Group 1: Haloperidol and vehicle (n= 6) (control)
Group 2: Haloperidol + compound 0.1 mg/kg (n = 6)
Group 3: Haloperidol + compound 0.4 mg/kg (n = 6)
Group 4: Haloperidol + compound 1 mg/kg (n = 6)
Group 5: Haloperidol + compound 2 mg/kg (n = 6)

In the catalepsy test in rats, statistical analysis was performed using a 1 way ANOVA test followed by Dunnett's multiple comparison's test for comparison between the control group and compound-treated groups. A probability of $p < 0.05$ was used to declare statistically significant differences.

4.7.3 Results

From the graphs below (Figure 4.13), it can be seen that the control group (cataleptic group), that received haloperidol alone, remained on the bar longer than the groups that received the different concentrations of KW 6002 (the known A_{2A} antagonist) and compounds **2m** and **2k**. For compound **2m,** a significant reduction in catalepsy was observed (as for KW 6002), even at the lowest dose of 0.1 mg/kg. However for compound **2k**, a significant reduction in catalepsy was only observed from the highest two doses (1- and 2 mg/kg). This is most likely due to the weaker affinity observed for compound **2k** in the A_{2A} binding assay.

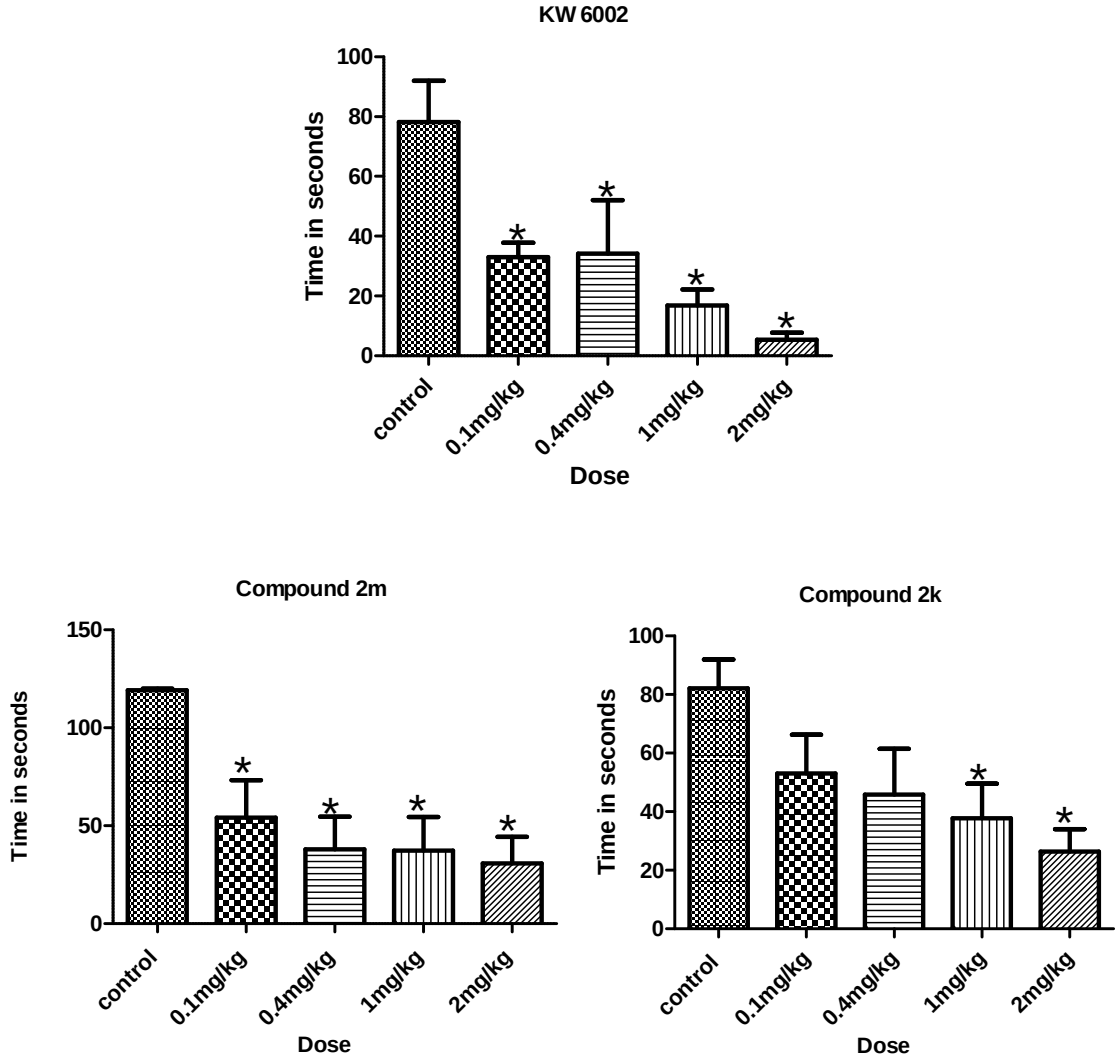

Figure 4.13: Graphs illustrating reversal of catalepsy with increased concentrations of KW 6002 as well as compounds **2m** and **2k**. * One way ANOVA followed by Dunnet's multiple comparison test $p < 0.05$.

The results obtained with compounds **2m** and **2k** are thus similar to those obtained with KW 6002, as well as those obtained with other adenosine A_{2A} antagonists (Antoniou *et al*., 2005; Kafka & Corbett, 1996; Malec, 1997; Moo-Puc *et al*., 2003), where catalepsy was reduced in the presence of the A_{2A} antagonist. It can therefore be concluded that compounds **2m** and **2k** are indeed adenosine A_{2A} antagonists.

4.8 Summary

In this chapter, the *in vitro* and *in vivo* biological evaluation of the synthesised chalcones and 2-aminopyrimidines were discussed. The chalcone intermediates (**1a** – **1h**) were screened for MAO-A and -B inhibitory activity using a fluorescence assay with kynuramine as substrate and the IC_{50} values were determined. The results from this assay suggest that these chalcones possess relative good selectivity and inhibitory activity for the MAO-B enzyme, making these compounds good leads for the future design of MAO-B inhibitors.

The reversibility and mode of inhibition was further investigated for compound (**1c**). The results obtained from these assays suggest that binding of compound **1c** to the MAO-B enzyme is reversible and competitive.

The affinities of the synthesised 2-aminopyrimidines for the adenosine A_{2A} receptor were also evaluated with a radioligand binding assay. The results show that derivatives **2j** - **2n** all had superior affinity for the A_{2A} receptor compared to derivatives **2a** - **2h**. Preliminary structure activity relationships could be derived from the data obtained, and the difference in affinities could at least partially be explained by docking experiments. The two most potent compounds (**2m** and **2k**) were selected to be evaluated in the haloperidol induced catalepsy assay. These compounds successfully reduced catalepsy and it was concluded that they are in fact antagonists of the adenosine A_{2A} receptor.